Available online at www.sciencedirect.com
ScienceDirect
Journal of Power Sources 175 (2008) 604–612
JOURNAL OF POWER SOURCES
www.elsevier.com/locate/jpowsour

Corrosion of Pb–Ca–Sn alloy during potential step cycles

Ken Sawai [a,*], Yuichi Tsuboi [a], Masashi Shiota [a], Nobumitsu Hirai [b], Shigeharu Osumi [a]

[a] *Technical Development Division, Automotive Battery Business Unit, GS Yuasa Power Supply Ltd., Nishinosho, Kisshoin, Minami-ku, Kyoto 601-8520, Japan*

[b] *Division of Materials and Manufacturing Science, Graduate School of Engineering, Osaka University, Osaka, Japan*

Received 16 July 2007; received in revised form 28 August 2007; accepted 29 August 2007
Available online 7 September 2007

Abstract

Potential step was applied to Pb–Ca–Sn alloy electrode at various potential and time regimes. No severe corrosion was observed during potential step cycle with cathodic potential under −140 mV or over −40 mV versus Pb/$PbSO_4$ (3.39 M H_2SO_4), or at constant potential without stepping. On the other hand, the Pb–Ca–Sn alloy was severely corroded during potential step with cathodic potential from −120 mV to −60 mV and with anodic potential of +40 mV or more positive. The corrosion could not be decreased with periodical rest at 0 mV, while it could be decreased with periodical reduction at high polarization of, e.g. −160 mV. It was found out that the severe corrosion occurs when the oxidation of Pb to $PbSO_4$ and partial reduction of passive film of $PbSO_4$ take turns many times.

Keywords: Lead-acid battery; Negative electrode; Corrosion; Passivation

1. Introduction

It is well known that positive lead alloy parts in lead-acid batteries, for example positive posts, straps, plate-lugs or grids, are often suffered by corrosion [1–3]. These parts tend to be easily corroded because of its high potential in sulfuric acid electrolyte, but are corroded much slower than other metal since the corrosion layer of PbO_2 forms passive film [1,2]. On the other hand, negative parts are not suffered from so high potential as positive parts. Negative electrode potential is more negative than Pb/$PbSO_4$ equilibrium potential during charging, therefore, oxidation of negative parts and negative active mass does not progress. Recently, however, some cases have been reported where negative parts out of electrolyte are suffered by corrosion [4–6]. It is because the equilibrium potential of metal Pb oxidation to $PbSO_4$ is more negative than the potential of H_2 evolution on negative electrode. Pb metal is corroded much slower in the electrolyte also at the potential of negative electrode of lead-acid battery, since the corrosion layer of $PbSO_4$ forms passive film [3].

Under specific potential conditions in the electrolyte, however, it has been found that Pb alloy can be easily corroded during potential step cycles around Pb/$PbSO_4$ equilibrium potential. Therefore, potential step cycle tests were performed at various anodic and cathodic potential of Pb alloy electrode to investigate the corrosion characteristics. The amount of corrosion layer formed during the cycle was measured and the results are compared with that of constant potential corrosion test.

The electrode surface during the potential step cycles was observed by in situ electrochemical atomic force microscope (EC-AFM) [7–11] to investigate the corrosion mechanisms. This observation technique is very useful for studying the electrode reactions in detail, because it can observe the electrode surface in sulfuric acid electrolyte directly. Various types of knowledge about the electrochemical reactions on the negative and positive electrodes of lead-acid batteries have been obtained through EC-AFM observation of the morphological changes on Pb and PbO_2 electrodes in sulfuric acid solution during oxidation and reduction.

2. Experimental

2.1. Potential-controlled corrosion test

First, mass loss of Pb alloy working electrode during potential step test and constant potential test was measured.

* Corresponding author. Tel.: +81 75 312 2123; fax: +81 75 316 3798.
E-mail address: ken.sawai@jp.gs-yuasa.com (K. Sawai).

0378-7753/$ – see front matter © 2007 Elsevier B.V. All rights reserved.
doi:10.1016/j.jpowsour.2007.08.109

A three-electrode cell was assembled. Working electrode was Pb–0.06 mass% Ca–0.6 mass% Sn alloy rolled sheet. The electrode surface area was 24 cm^2 for both sides. Counter electrode was Pb sheet with 120 cm^2 for both sides. Reference electrode was $Pb/PbSO_4$ (3.39 M H_2SO_4). The reference electrode was prepared as follows. Leady oxide powder (the row material of lead-acid battery active mass) and water and sulfuric acid was mixed to a paste, and the paste was put on Pb metal wire. The paste was reduced to sponge Pb in H_2SO_4 solution, washed and dried, and soaked into 3.39 M H_2SO_4. Mass of the sponge Pb was ca. 1 g, and BET surface area of the reference electrode was 3000–5000 cm^2 g. The test cell and the reference electrode were connected via bridge of silica gel and H_2SO_4. The potential of reference electrodes was checked each other at every test, and it was stable enough during these tests. It may be because enough surface area of the electrode. All the potentials described below are referred to this electrode. Electrolyte was 3.39 M H_2SO_4 aqueous solution.

The working electrodes were prepared by cathodic reduction in the cell at 30 mA for 2 h in 3.39 M H_2SO_4 at 40 °C. Potential regime of the working electrodes in corrosion test will be shown in Sections 2.1.1 and 2.1.2. Test period was 168 h, and ambient temperature was 40 °C.

The working electrode after the corrosion test was rinsed with distilled water and the corrosion layer was removed by alkaline mannitol solution. Mass of the working electrode before the corrosion test and after elimination of the corrosion layer was measured and the mass loss was calculated.

2.1.1. Potential step corrosion test

Potential step corrosion tests were performed under conditions as follows.

Cycle regime was set to repeat step at anodic potential for 30 s and cathodic potential for 30 s alternately. The cycle was repeated for 168 h (10,080 cycles).

Test A: The test regime is shown in Fig. 1. Anodic potential was set at +40 mV, and cathodic potential was changed to investigate the potential region for severe corrosion, at 0 mV, −20 mV, −40 mV, −60 mV, −80 mV, −100 mV, −120 mV, −140 mV and −160 mV.

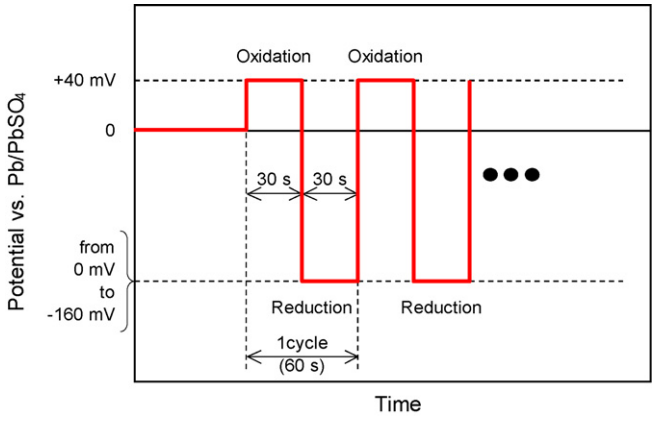

Fig. 1. Potential profile of working electrode in the potential step test A to measure mass loss by corrosion.

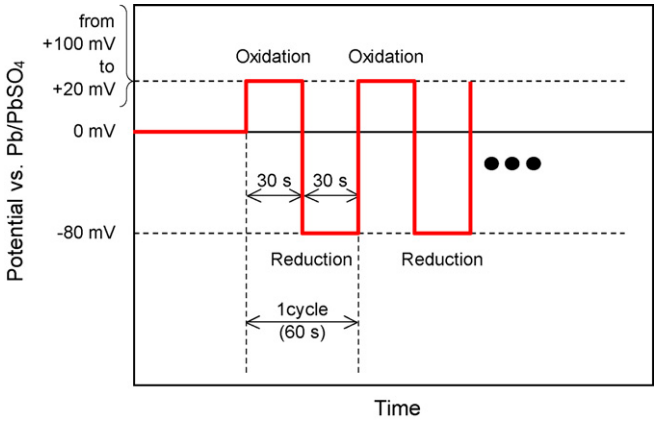

Fig. 2. Potential profile of working electrode in the potential step test B to measure mass loss by corrosion.

Test B: The test regime is shown in Fig. 2. Cathodic potential was set at −80 mV and anodic potential was changed at +20 mV, +40 mV, +70 mV, and +100 mV.

Test C: The test regime is shown in Fig. 3. The cycle regime was changed. Step interval at +40 mV anodic potential and −80 mV cathodic potential was changed for 15 s, 30 s, 45 s, and 60 s. Time for one cycle during these tests was 30 s, 60 s, 90 s, and 120 s, respectively.

Test D: The test regime is shown in Fig. 4. The rest at 0 mV was taken for 1 h or 2 h every 60 cycles of 30 s interval steps. These potential step cycles were also repeated for 168 h, and test cycles were changed due to each regime.

Test E: The test regime is shown in Fig. 5. More negative potential step at −160 mV was taken for 180 s with various frequencies. The frequency of the potential step at −160 mV was set at once per 20 min, 30 min, 1 h, and 2 h. They correspond to step at −160 mV every 17, 27, 57 and 117 cycles, respectively. These potential step cycles were also repeated for 168 h, and test cycles were changed due to each regime.

2.1.2. Constant potential corrosion test

The working electrodes were kept for 168 h at +20 mV, +30 mV, +40 mV, +50 mV and +60 mV. These potentials cor-

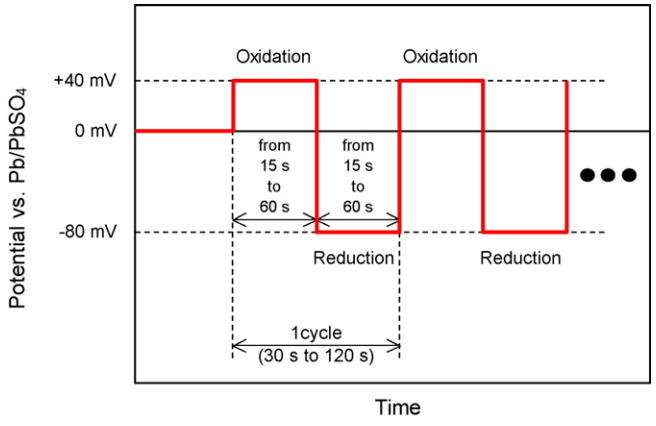

Fig. 3. Potential profile of working electrode in the potential step test C to measure mass loss by corrosion.

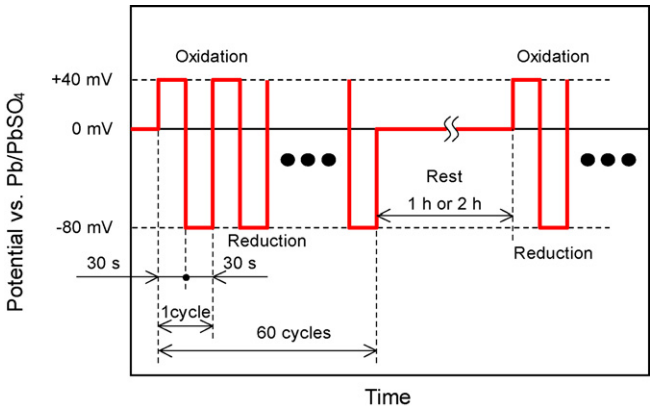

Fig. 4. Potential profile of working electrode in the potential step test D to measure mass loss by corrosion.

respond to negative electrode potential during continuous discharge in a lead-acid battery.

2.2. *In situ electrochemical atomic force microscope (EC-AFM) observation during potential step*

In situ EC-AFM observation [7–11] was performed to investigate corrosion mechanisms.

Fig. 6 shows schematic illustration of the EC-AFM measurement. Working electrodes were Pb alloy rolled sheet. They were 100 mm in length, 20 mm in width. The alloy composition was Pb–0.06 mass% Ca–0.6 mass% Sn. Counter electrode was PbO_2 and reference electrode was Hg/Hg_2SO_4 (0.5 M H_2SO_4). The electrode potential will be converted to voltage versus $Pb/PbSO_4$ (3.39 M H_2SO_4) in convenience.

Electrolyte was 3.39 M H_2SO_4 aqueous solution.

2.2.1. *Electrode preparation*

Surface of working electrode was polished with abrasive papers and then buffed with fine Al_2O_3 powder. Next, the electrode surface was polished chemically with a mixed solution of acetic acid and hydrogen peroxide, rinsed with distilled water, substituted with ethanol, and finally dried.

The working electrode was assembled into the EC-AFM cell, and then the cell was filled with 3.39 M sulfuric acid electrolyte.

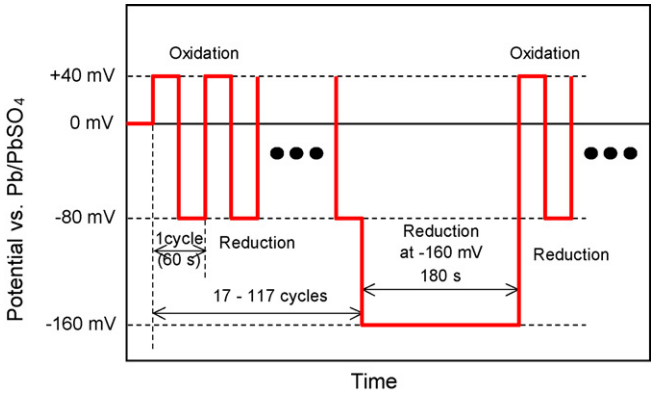

Fig. 5. Potential profile of working electrode in the potential step test E to measure mass loss by corrosion.

The electrode was reduced by two steps of potential, starting at −390 mV for 10 min followed by −190 mV for 10 min, to remove lead sulfate from the surface.

2.2.2. *EC-AFM observation*

Electrode surface morphology was observed by EC-AFM immediately after sample preparation. Fig. 7 shows time schedule for the EC-AFM observation and electrode potential step. Time for oxidation or reduction was 30 s, and the rest time for EC-AFM observation was 60 s. Cycle regime was varied to compare the surface morphology of the working electrode during cycling. The oxidation potential was set at +40 mV, and the reduction potential was set at −200 mV, −80 mV, and −20 mV. The same region of the electrode was observed in every cycle for each sample. The temperature was 25 °C through the whole experiment. The observed area for an AFM image was 10 μm × 10 μm, its mode was deflection mode, and its time per one image was 52 s.

3. Results and discussion

3.1. *Potential-controlled corrosion test*

3.1.1. *Potential step corrosion test*

Test A: Fig. 8 shows the mass loss of working electrode by corrosion during the potential step cycle. Working electrode was severely corroded at cathodic potential from −60 mV to −120 mV. Corrosion of working electrode was less when the cathodic potential of cycle was more positive than −60 mV or more negative than −120 mV. The maximum mass loss was 145 mg cm^2 during 168-h cycles at −80 mV cathodic potential. Corrosion layer of $PbSO_4$ cannot prevent the electrode surface from further oxidation during the specific potential step. Then the structure of the corrosion layer was observed. Fig. 9 shows photograph of the working electrode and corrosion layer in cross-section of the sample, after potential step cycles between +40 mV and −80 mV. The corrosion layer was made of $PbSO_4$. It shows that the corrosion layer was porous and uniform, unlike the grain boundary corrosion at the positive grid. It shows that the electrode repeated dissolution and precipitation and passive layer of dense $PbSO_4$ is not formed under these conditions. The corrosion layer was 0.4 mm thick measured from Fig. 9. The 145 mg cm^2 mass loss of the electrode is corresponding to 0.128 mm depth of corrosion on Pb alloy electrode surface. The volume becomes 3.1 times from 0.128 mm to 0.4 mm after the corrosion, because the density of $PbSO_4$ is lower than that of Pb metal, and the corrosion layer is porous.

Test B: Fig. 10 shows the mass loss of working electrode by corrosion during the potential step cycle with various anodic potential. Mass loss of electrode increased steeply at +40 mV anodic potential and remained at almost the same level when the anodic step potential was more positive than +40 mV. It shows that malfunction of passive layer against the corrosion is caused by the specific cathodic potential during cycling, and not by the anodic potential.

Test C: Fig. 11 shows the mass loss of working electrode by corrosion during the potential step cycle with various inter-

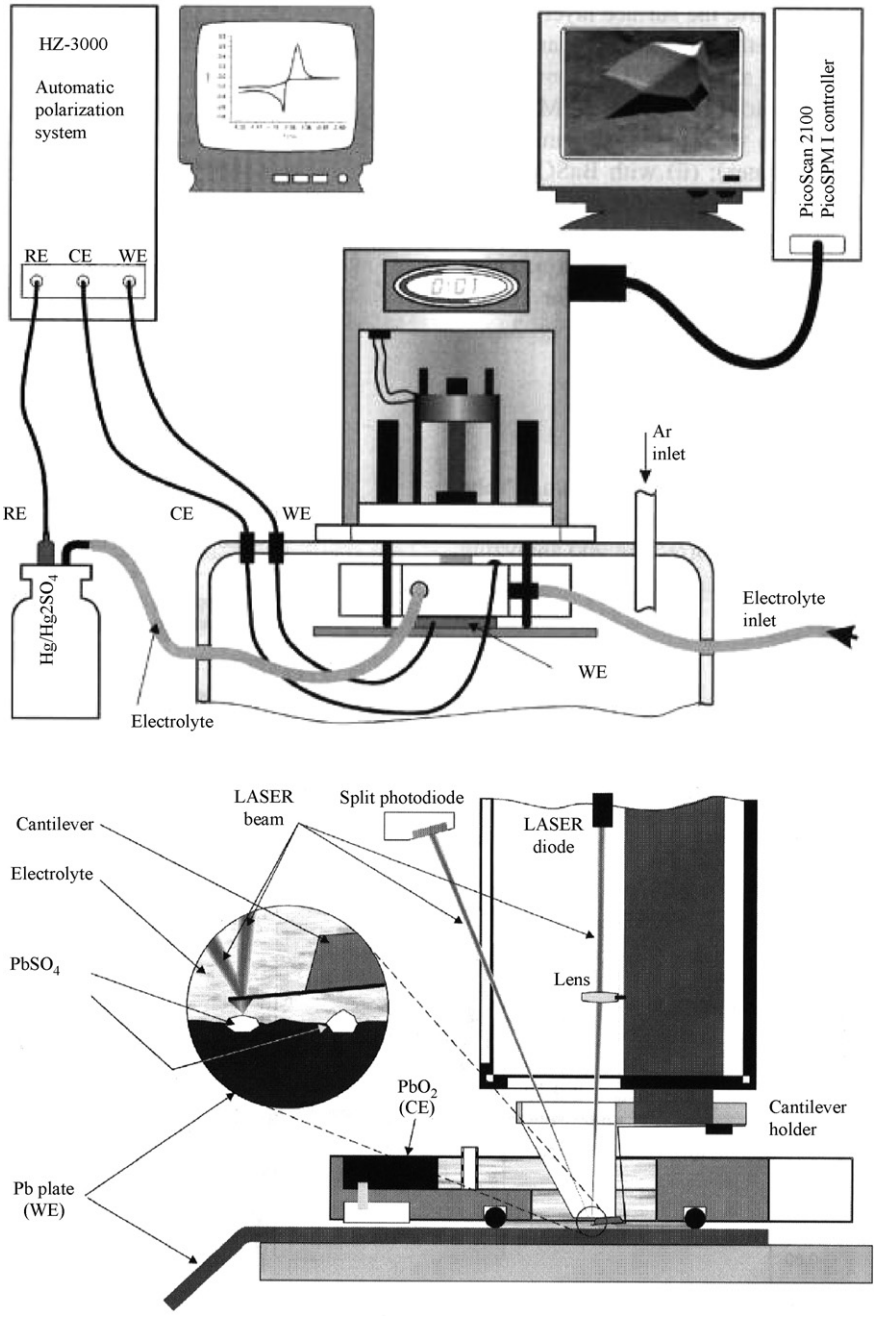

Fig. 6. Schematic of the EC-AFM apparatus.

vals. Mass loss of electrode during 168 h was increased with shorter step interval. The mass loss during 10,080 cycles of each step interval was calculated from the data. It was increased with longer step interval.

Test D: Fig. 12 shows the mass loss of working electrode by corrosion during the potential step cycle with no rest or with 1 h or 2 h rest, for every 60 cycles. Although the mass loss of electrode during 168 h was decreased with longer rest, the mass loss during 10,080 cycles calculated from the data was almost the same under these conditions. It shows that the corrosion rate is not affected by the rest during the cycles but is determined by time and number of steps between anodic and cathodic potential steps during cycles. Function of $PbSO_4$ layer against further corrosion of the surface does not change during the rest.

Test E: Fig. 13 shows the mass loss of working electrode by corrosion during the potential step cycle with reduction step at −160 mV for 180 s with various frequencies. The mass loss of electrode was decreased with more frequent reduction at −160 mV. It shows that corrosion layer formed during the oxidation–reduction cycles is reduced to metal Pb during cathodic polarization at −160 mV and corrosion do not advance.

3.1.2. Constant potential corrosion test

Fig. 14 shows the mass loss of working electrode by corrosion during the constant potential corrosion test.

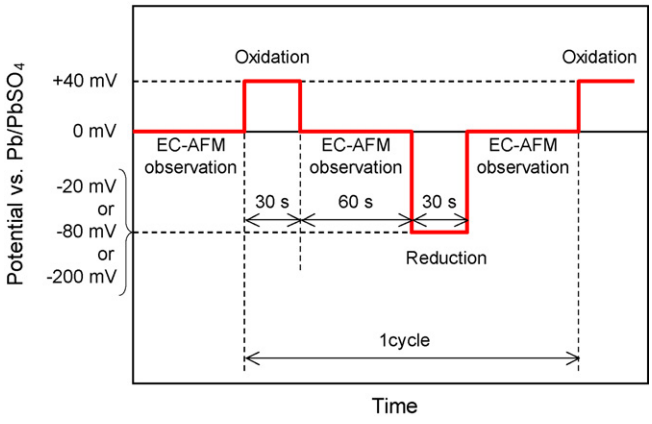

Fig. 7. Potential profile of working electrode to observe surface morphology by EC-AFM during potential step test.

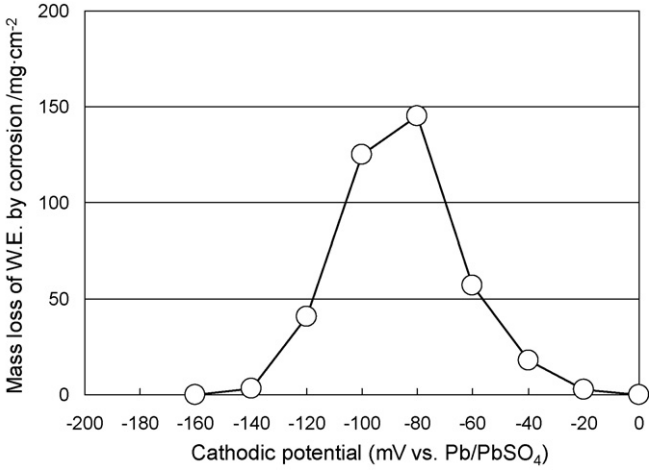

Fig. 8. Mass loss of working electrode during potential step corrosion test at various cathodic potential.

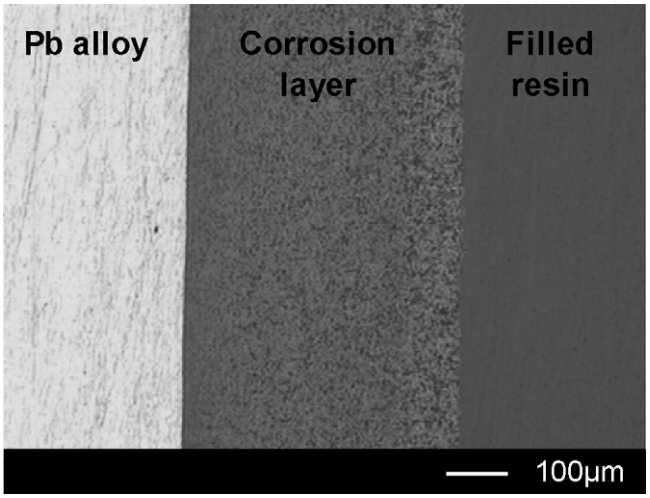

Fig. 9. The SEM photograph of cross-section of the working electrode after potential step test.

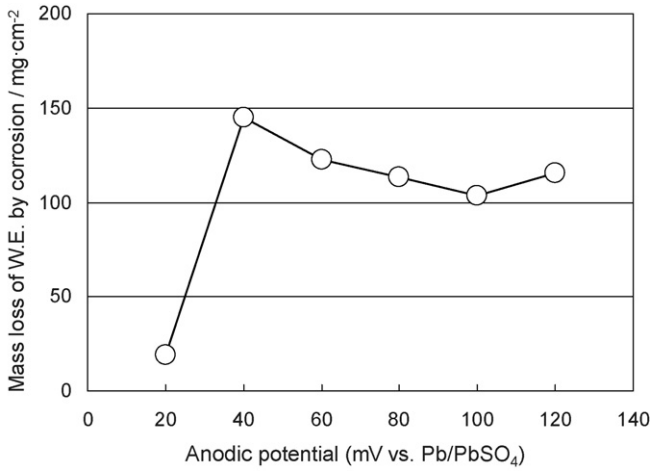

Fig. 10. Mass loss of working electrode during potential step corrosion test at various anodic potential.

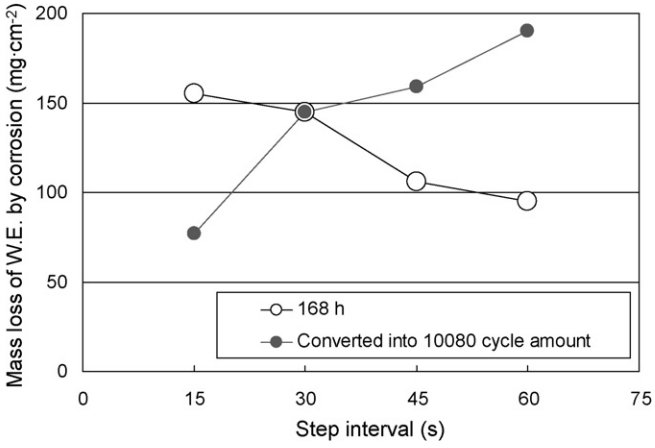

Fig. 11. Mass loss of working electrode during potential step corrosion test with various step intervals.

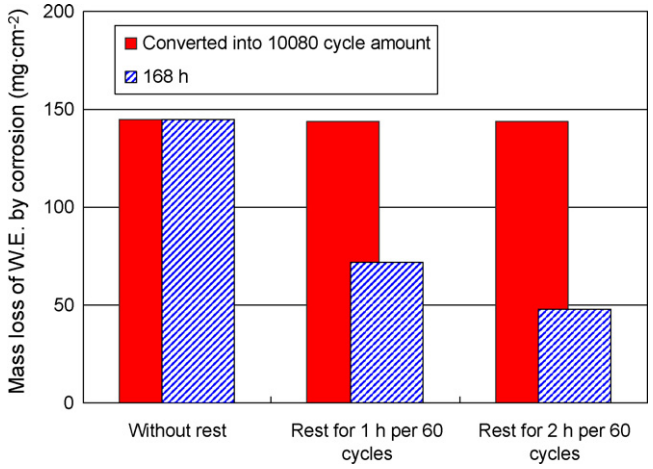

Fig. 12. Mass loss of working electrode during potential step corrosion test with rest for various periods.

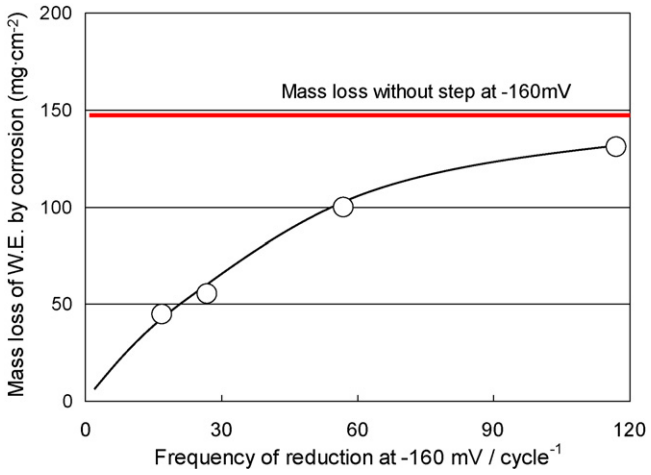

Fig. 13. Mass loss of working electrode during potential step corrosion test with cathodic polarization at −160 mV for 180 s at various frequencies.

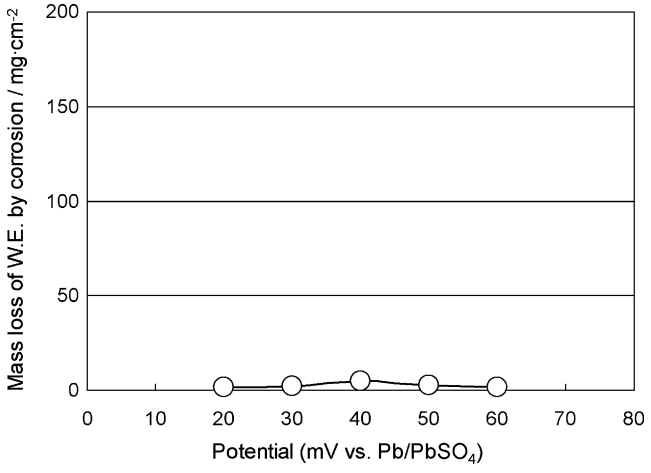

Fig. 14. Mass loss of working electrode during constant potential corrosion test at various potential.

Corrosion of working electrode was not so severe than those of potential step tests. Corrosion layer did not develop with constant anodic potential. It is supposed that dense passive layer of $PbSO_4$ is formed on the electrode. It shows that the corrosion advances only when the potential is stepped to the specific cathodic potential.

3.2. *In situ AFM observation during potential step*

Fig. 15 shows the EC-AFM images of electrode surface at initial state (Fig. 15(a)), after oxidation at +40 mV (Fig. 15(b)) and after reduction at −200 mV (Fig. 15(c)) of the same part of the working electrode surface at the first cycle.

At the initial state, the AFM image (Fig. 15(a)) shows the surface of Pb alloy. After the first oxidation, smooth particles of 5 μm or more covered the electrode surface (Fig. 15(b)). It shows that $PbSO_4$ particles were formed by oxidation on the surface. Then, after the first reduction, the particles disappeared (Fig. 15(c)). The surface image after the reduction is similar to that at the initial state (Fig. 15(a) and (c)). It shows that $PbSO_4$ particles on the surface were reduced to Pb. It is found out that $PbSO_4$ particles formed at anodic potential disappear at cathodic potential.

Fig. 16 shows the EC-AFM images of electrode surface during potential step between +40 mV and −200 mV. The images were taken before the seventh cycle (Fig. 16(a)), and after oxidation at +40 mV (Fig. 16(b)) and after reduction at −200 mV (Fig. 16(c)) at the seventh cycle.

The surface image before the seventh cycle (Fig. 16(a)) is similar to that at the initial state (Fig. 15(a)). Particles, which were supposed to be $PbSO_4$, covered the electrode surface after oxidation at +40 mV (Fig. 16(b)), and they disappeared after reduction at −200 mV (Fig. 16(c)). Appearance of electrode surface seemed not to be changed before (Fig. 16(a)) and after the seventh cycle (Fig. 16(c)). It shows that $PbSO_4$ formed at anodic potential is reduced to metal Pb at −200 mV for 30 s in every cycles and corrosion do not advance further.

Fig. 17 shows the EC-AFM images of electrode surface during potential step between +40 mV and −80 mV. The images were taken before the seventh cycle (Fig. 17(a)), after oxidation at +40 mV (Fig. 17(b)) and after reduction at −80 mV (Fig. 17(c)) at the seventh cycle.

The electrode surface was already partially covered with smooth particles of $PbSO_4$ (Fig. 17(a)). After oxidation (Fig. 17(b)), more $PbSO_4$ particles were formed at lower center and upper left corner of image, and the particle at left side grew larger. After the reduction (Fig. 17(c)), the particle at lower center disappeared. However, the particle at left side did not disappeared or seemed grown more, and the particles at upper left corner changed the shape and also did not disappeared. The electrode surface was covered more with $PbSO_4$ particles after

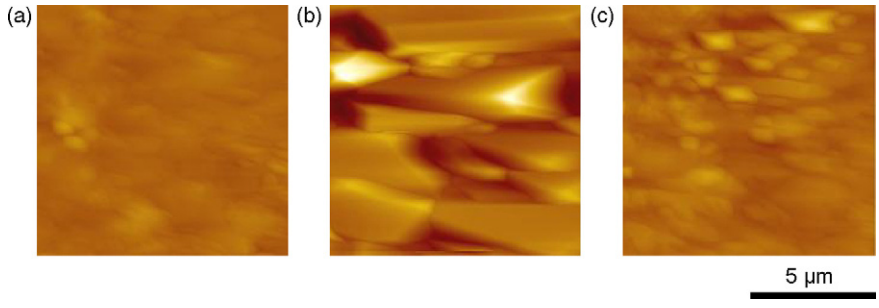

Fig. 15. The EC-AFM images of working electrode surface: (a) at the initial state; (b) after oxidation at +40 mV at the first cycle; (c) after reduction at −200 mV at the first cycle; of potential step test. Side length of the photographs is 10 μm.

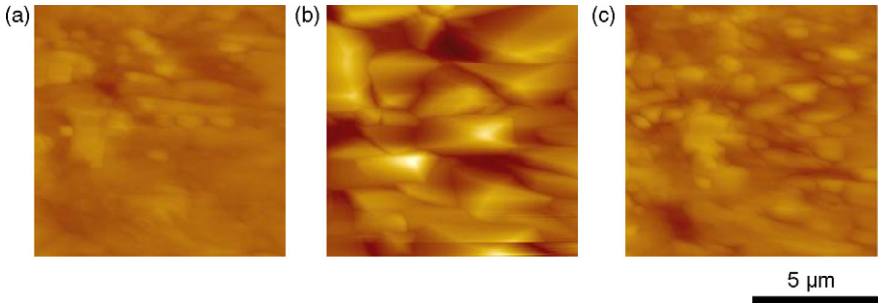

Fig. 16. The EC-AFM images of working electrode surface: (a) before oxidation at the seventh cycle; (b) after oxidation at +40 mV at the seventh cycle; (c) after reduction at −200 mV at the seventh cycle; of potential step test. Side length of the photographs is 10 μm.

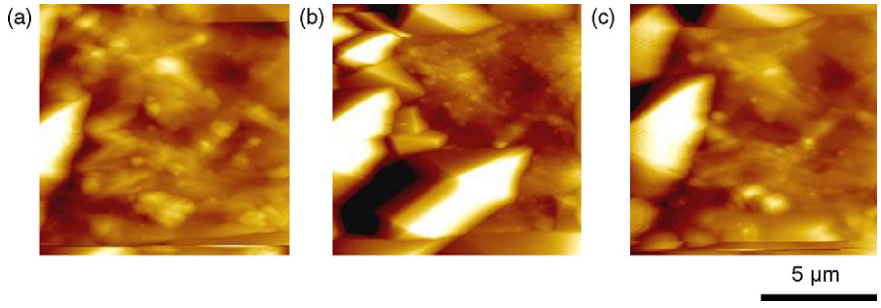

Fig. 17. The EC-AFM images of working electrode surface: (a) before oxidation at the seventh cycle; (b) after oxidation at +40 mV at the seventh cycle; (c) after reduction at −80 mV at the seventh cycle; of potential step test. Side length of the photographs is 10 μm.

(Fig. 17(c)) the seventh cycle than before (Fig. 17(a)). It was found out that $PbSO_4$ formed at anodic potential is not fully reduced to metal Pb at −80 mV for 30 s in every cycles and corrosion advances. Each $PbSO_4$ particle is not equally reduced, and some $PbSO_4$ particles are reduced to Pb and the other remained unreduced at −80 mV. $PbSO_4$ particles accumulate on the surface unevenly, and during repetition, porous corrosion layer is formed at the surface. Unreduced $PbSO_4$ particles could not be distinguished from reduced particles by their size or shape by the image (Fig. 17(b) and (c)). Other conditions like sulfuric acid concentration or local current density may affect reactivity.

Fig. 18 shows the EC-AFM images of electrode surface during potential step between +40 mV and −20 mV. The images were taken before the seventh cycle (Fig. 18(a)), after oxidation at +40 mV (Fig. 18(b)) and after reduction at −20 mV (Fig. 18(c)) at the seventh cycle.

The electrode surface was already covered firmly with $PbSO_4$ particles (Fig. 18(a)), and little change was observed during the seventh cycle (Fig. 18(b) and (c)). The $PbSO_4$ particles seem to form passive layer and it cannot be reduced during step at −20 mV.

3.3. Mechanism of corrosion of Pb–Ca–Sn alloy during potential step

Fig. 19 shows the schematic diagram of the corrosion mechanism during potential step cycles with various reduction potentials.

When the reduction potential is −200 mV, $PbSO_4$ formed at +40 mV is fully reduced at −200 mV for 30 s in every cycle and $PbSO_4$ does not accumulate.

The severe corrosion observed during the potential step cycle is caused by repetition of oxidation and reduction of Pb

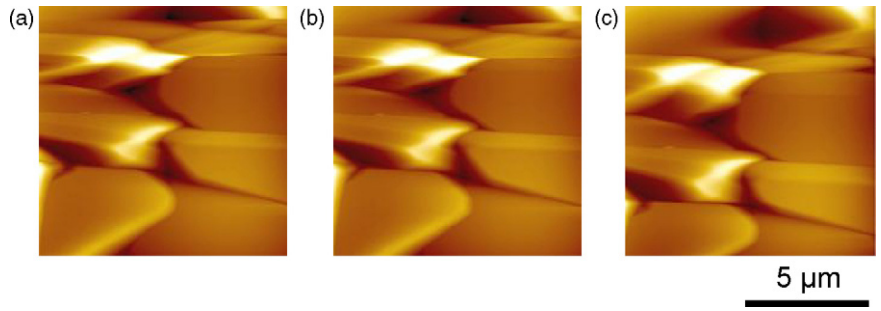

Fig. 18. The EC-AFM images of working electrode surface: (a) before oxidation at the seventh cycle; (b) after oxidation at +40 mV at the seventh cycle; (c) after reduction at −20 mV at the seventh cycle; of potential step test. Side length of the photographs is 10 μm.

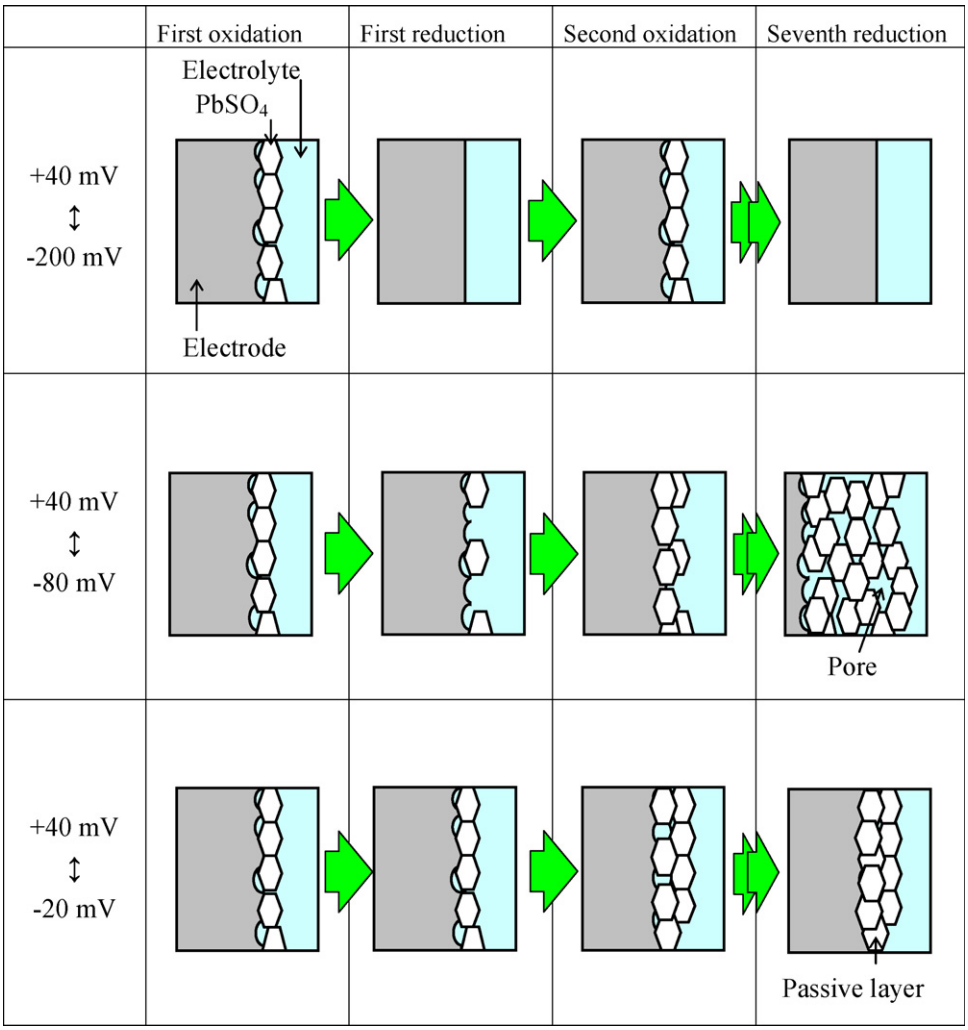

Fig. 19. Schematic diagram of corrosion mechanism during potential step cycles with various reduction potentials.

alloy. When the electrode potential is stepped between +40 mV and −80 mV, $PbSO_4$ formed at +40 mV is not fully reduced at −80 mV for 30 s and $PbSO_4$ accumulates gradually. Some of the $PbSO_4$ particles are reduced and the corrosion layer become porous, sulfuric acid can go into the deeper electrode surface, and the corrosion advances at the next +40 mV step.

When the reduction potential is −20 mV, $PbSO_4$ formed at +40 mV is not reduced at −20 mV for 30 s and $PbSO_4$ forms dense passive layer like constant potential corrosion.

The corrosion rate is depend on the number of partial reduction times of passive layer, or cycle number, therefore, the rate is not lowered by the rest at 0 mV or longer step interval for the same cycle number.

On the other hand, frequent cathodic polarization at −160 mV for 180 s is effective to decrease the thickness of corrosion layer. Even if the corrosion layer is developing, it can be reduced to metal Pb at −160 mV.

Some of $PbSO_4$ particles can be reduced to Pb and some remain at −80 mV, therefore $PbSO_4$ accumulates on the electrode surface but passive layer is broken at each cycle. That causes the porous thick corrosion layer on the surface.

4. Conclusions

Potential step was applied to Pb–Ca–Sn alloy electrode at various potential and time regimes. No severe corrosion was observed with cathodic potential under −140 mV or over −20 mV versus $Pb/PbSO_4$ (3.39 M H_2SO_4), or at constant potential without potential step. On the other hand, the Pb–Ca–Sn alloy was severely corroded during potential step cycles when the cathodic potential was from −120 mV to −40 mV for 30 s and the anodic potential was +40 mV or more positive for 30 s. The corrosion could not be decreased with periodical rest at 0 mV, while it could be decreased with periodical reduction at high polarization, e.g. −160 mV. It was found out that the severe corrosion occurs when the oxidation of Pb to $PbSO_4$ and partial reduction of $PbSO_4$ passive film take turns many times.

References

[1] P. Ruetschi, J. Power Sources 127 (2004) 33.
[2] D. Berndt, Handbook of Battery Technology, 2nd ed., Research Studies Press Ltd., Taunton, England, 1997, p. 153.

[3] H. Bode, Lead-acid Batteries (Transl. R.J. Brodd, K. Kodesch), Wiley, New York, 1977, p. 338.
[4] D. Berndt, Handbook of Battery Technology, 2nd ed., Research Studies Press Ltd., Taunton, England, 1997, p. 164.
[5] T. Omae, S. Osumi, K. Takahashi, M. Tsubota, J. Power Sources 65 (1996) 65.
[6] N. Koura, K. Kasuya, K. Ui, Y. Takiguchi, Y. Idemoto, Electrochemistry 73 (2005) 135.
[7] Y. Yamaguchi, M. Shiota, Y. Nakayama, N. Hirai, S. Hara, J. Power Sources 85 (2000) 22.
[8] Y. Yamaguchi, M. Shiota, Y. Nakayama, N. Hirai, S. Hara, J. Power Sources 93 (2001) 104.
[9] Y. Yamaguchi, M. Shiota, M. Hosokawa, Y. Nakayama, N. Hirai, S. Hara, J. Power Sources 102 (2001) 155.
[10] N. Hirai, D. Tabayashi, M. Shiota, T. Tanaka, J. Power Sources 133 (2004) 32.
[11] H. Vermesan, N. Hirai, M. Shiota, T. Tanaka, J. Power Sources 133 (2004) 52.